

Inhibition of De Novo Ceramide Synthesis Reverses Diet-Induced Insulin Resistance and Enhances Whole-Body Oxygen Consumption

John R. Ussher,¹ Timothy R. Koves,² Virgilio J.J. Cadete,¹ Liyan Zhang,¹ Jagdip S. Jaswal,¹ Suzanne J. Swyrd, David G. Lopaschuk,¹ Spencer D. Proctor,³ Wendy Keung,¹ Deborah M. Muoio,² and Gary D. Lopaschuk¹

OBJECTIVE—It has been proposed that skeletal muscle insulin resistance arises from the accumulation of intramyocellular lipid metabolites that impede insulin signaling, including diacylglycerol and ceramide. We determined the role of de novo ceramide synthesis in mediating muscle insulin resistance.

RESEARCH DESIGN AND METHODS—Mice were subjected to 12 weeks of diet-induced obesity (DIO), and then treated for 4 weeks with myriocin, an inhibitor of serine palmitoyl transferase-1 (SPT1), the rate-limiting enzyme of de novo ceramide synthesis.

RESULTS—After 12 weeks of DIO, C57BL/6 mice demonstrated a doubling in gastrocnemius ceramide content, which was completely reversed (141.5 ± 15.8 vs. 94.6 ± 10.2 nmol/g dry wt) via treatment with myriocin, whereas hepatic ceramide content was unaffected by DIO. Interestingly, myriocin treatment did not alter the DIO-associated increase in gastrocnemius diacylglycerol content, and the only correlation observed between lipid metabolite accumulation and glucose intolerance occurred with ceramide ($R = 0.61$). DIO mice treated with myriocin showed a complete reversal of glucose intolerance and insulin resistance which was associated with enhanced insulin-stimulated Akt and glycogen synthase kinase $\beta 3$ phosphorylation. Furthermore, myriocin treatment also decreased intramyocellular ceramide content and prevented insulin resistance development in *db/db* mice. Finally, myriocin-treated DIO mice displayed enhanced oxygen consumption rates ($3,041 \pm 124$ vs. $2,407 \pm 124$ ml/kg/h) versus their control counterparts.

CONCLUSIONS—Our results demonstrate that the intramyocellular accumulation of ceramide correlates strongly with the development of insulin resistance, and suggests that inhibition of SPT1 is a potentially promising target for the treatment of insulin resistance. *Diabetes* 59:2453–2464, 2010

From the ¹Cardiovascular Research Centre, Mazankowski Alberta Heart Institute, Department of Pediatrics, University of Alberta, Edmonton, Canada; the ²Sarah W. Stedman Nutrition and Metabolism Center, Department of Medicine, Duke University, Durham, North Carolina; and the ³Metabolic and Cardiovascular Diseases Laboratory, Alberta Institute for Human Nutrition, University of Alberta, Edmonton, Canada.

Corresponding author: Gary Lopaschuk, gary.lopaschuk@ualberta.ca. Received 31 August 2009 and accepted 5 May 2010. Published ahead of print at <http://diabetes.diabetesjournals.org> on 3 June 2010. DOI: 10.2337/db09-1293.

© 2010 by the American Diabetes Association. Readers may use this article as long as the work is properly cited, the use is educational and not for profit, and the work is not altered. See <http://creativecommons.org/licenses/by-nc-nd/3.0/> for details.

The costs of publication of this article were defrayed in part by the payment of page charges. This article must therefore be hereby marked "advertisement" in accordance with 18 U.S.C. Section 1734 solely to indicate this fact.

See accompanying commentary, p. 2351.

Obesity and type 2 diabetes frequently occur hand in hand, and are thought of as diseases of Western society, due to lifestyles characterized by overnutrition and physical inactivity. This overnutrition manifests itself as hyperlipidemia, which is believed to be a major precipitating event in the development of skeletal muscle insulin resistance (1,2).

Numerous studies in vivo and in vitro have provided strong evidence that lipid excess leads to an accumulation of intramyocellular lipid-derived metabolites, which coincide with an impaired insulin response (3,4). Previous studies have postulated that this accumulation of lipid-derived metabolites results from an impaired ability of the mitochondria to oxidize fatty acids (5–8). Thus, esterified fatty acids in the form of long-chain acyl-CoA are diverted away from carnitine palmitoyl transferase 1, the rate-limiting enzyme in the mitochondrial uptake and oxidation of fatty acids, toward triacylglycerol (TAG) and other lipid metabolites, such as ceramide and diacylglycerol (DAG). These metabolites are believed to activate classic/novel protein kinase C isoforms that phosphorylate and inactivate insulin receptor substrate proteins, preventing the insulin response at the level of Akt and GLUT4 translocation (3,4).

Of the aforementioned lipid metabolites, ceramide is an attractive candidate to be a primary culprit involved in mediating the skeletal muscle insulin resistance seen with obesity and type 2 diabetes, as it is elevated by both inflammation and nutrient overload, and hence links two popular models of insulin-resistance development (9). Numerous studies in both culture and animal models demonstrate that increasing ceramide levels inhibit insulin signaling and cause insulin resistance (10–13). Moreover, Holland et al. showed that inhibiting de novo synthesis of ceramide by pharmacological inhibition of serine palmitoyl transferase one (SPT1) can prevent insulin resistance caused by corticosteroids, saturated fats, and genetic models of obesity (12). Pharmacological inhibition of SPT1 in human muscle cells has also been shown to prevent the inhibition of insulin-stimulated glycogen synthesis induced by palmitic acid (11). Finally, improvements in insulin sensitivity brought about by exercise training in obese patients are associated with significant reductions in intramyocellular ceramide levels, whereas TAG and DAG levels were either unchanged or showed only a trend to a reduction (14,15).

Our objective in this investigation was to determine if inhibition of de novo ceramide synthesis could reverse the

TABLE 1

β -hydroxyacyl-CoA dehydrogenase (β HAD) activity in gastrocnemius muscle of lean and obese mice treated with vehicle control or myriocin

	LF Control	LF myriocin	HF control	HF myriocin
β HAD activity	3.05 \pm 0.29	3.19 \pm 0.52	4.28 \pm 0.31*	4.98 \pm 0.60*

Values reported are μ mol/g wet weight/min of $n = 5$ mice. Differences were determined using a two-way ANOVA followed by Bonferroni post hoc analysis. *Significantly different from the low-fat counterpart. LF, low-fat diet; HF, high-fat diet.

insulin resistance induced by chronic high-fat feeding of mice, and to gain a further understanding of how ceramides affect insulin sensitivity in muscle.

RESEARCH DESIGN AND METHODS

An expanded RESEARCH DESIGN AND METHODS section and supplementary figures can be found in an online data supplement available at <http://diabetes.diabetesjournals.org/cgi/content/full/db09-1293/DC1>. Details on glucose and insulin tolerance testing, plasma insulin level determination, lipid metabolite measurement, metabolomics, exercise capacity studies, whole-body in vivo metabolic assessment, and immunoblot analysis are provided in the online data supplement.

All animals received care according to the Canadian Council on Animal Care and the University of Alberta Health Sciences Animal Welfare Committee. Twelve-week-old C57BL/6 mice were placed on a standard chow/low-fat diet (4% kcal from lard) or high-fat diet (60% kcal from lard, Research Diets; D12492) for a 12-week period. At the end of week 12, animals were injected intraperitoneally every other day with the SPT1 inhibitors, myriocin (0.5 mg/kg) suspended in 1x PBS, L-cycloserine (25 mg/kg) suspended in 1x PBS, or vehicle control for a 4-week period. At the end of the 4-week treatment protocol, animals were killed via intraperitoneal injection of sodium pentobarbital (12 mg) in the fed state in the middle of the dark cycle. Tissues were excised and immediately frozen in liquid N₂. In another study, 6-week-old *db/db* mice and their heterozygous controls (*db/+*) (Jackson Laboratories) were placed on an identical 4-week treatment regimen.

RESULTS

Chronic high-fat feeding results in dramatic weight gain, whole-body insulin resistance, and altered substrate preference. As expected, mice fed a high-fat diet for 12 weeks became obese as indicated by a significant increase in weight gain, (supplementary Fig. 1A), and became insulin resistant (supplementary Fig. 1B–D). Diet-induced insulin-resistant and lean mice were placed in a comprehensive lab animal-monitoring system (CLAMS) for whole-body metabolic assessment, which demonstrated a high-fat diet-induced shift in fuel preference toward fatty acids as an oxidative energy source, indicated by the large drop in the respiratory exchange ratio (RER) (supplementary Fig. 2A and B). Further support for an increase in fatty acid oxidation in obese mice is seen with the increase in gastrocnemius β -hydroxyacyl-CoA dehydrogenase (β HAD) activity (Table 1). Contrary to previous findings (16,17), we also report here that obesity induced by chronic high-fat feeding impairs whole-body oxygen consumption rates (supplementary Fig. 2C and D).

Inhibition of de novo ceramide synthesis via pharmacological inhibition of SPT1 reverses diet-induced insulin resistance. After 12 weeks of low- or high-fat diet, mice were treated with either myriocin (0.5 mg/kg every other day) or vehicle control. After 2 weeks of treatment, we demonstrated that inhibition of SPT1 with myriocin reverses diet-induced insulin resistance, as determined by glucose tolerance and insulin tolerance testing (Fig. 1A–D). To determine if these protective effects took place at the skeletal muscle level, a group of animals were killed at 30 min after insulin injection during the insulin tolerance test, and muscles were excised and harvested for immunoblot analysis of the insulin-signaling

pathway. We demonstrate that insulin stimulation of both Akt and glycogen synthase kinase 3 β (GSK3 β) phosphorylation were significantly improved in the gastrocnemius muscle of obese mice treated with myriocin (Fig. 1E and F). Phosphorylation of 5'AMP activated protein kinase (AMPK), another key signaling molecule regulating glucose metabolism, did not differ in gastrocnemius muscle of control and myriocin-treated obese mice (data not shown).

Myriocin treatment was without effect on food intake, body weight, and plasma insulin levels, but did reduce both postprandial and fasted plasma glucose levels in obese, insulin-resistant mice (Table 2). Although fasting plasma insulin levels did not differ between diet-induced obesity (DIO) mice treated with vehicle-control or myriocin, more sophisticated studies monitoring the changes in plasma insulin in response to a meal tolerance test in the obese JCR:LA cp rat illustrate a significant improvement in plasma insulin control after treatment with the SPT1 inhibitor, L-cycloserine (supplementary Fig. 3). Interestingly, indirect calorimetry revealed that the improved insulin sensitivity in DIO mice treated with myriocin was not associated with a decrease in fatty acid oxidation and an increase in carbohydrate oxidation, as similar RER values were observed between the DIO control and myriocin-treated animals (Fig. 2).

In a parallel series of experiments, after 12 weeks of high-fat feeding, mice were treated with either the SPT1 inhibitor, L-cycloserine (25 mg/kg every other day) or vehicle control. Although not as dramatic as the results observed with myriocin, at 2 weeks after treatment, we report improvements in glucose and insulin tolerance in mice treated with L-cycloserine (supplementary Fig. 4).

Inhibition of de novo ceramide synthesis via pharmacological inhibition of SPT1 reverses diet-induced impairments in exercise capacity, which coincide with a restoration of whole-body oxygen consumption rates and inhibition of fatty acid oxidation. Obese, insulin-resistant mice were run on an exercise treadmill to determine exercise capacity. As expected, obese mice showed a dramatic reduction in both their treadmill time and distance when compared with their lean counterparts (Fig. 3A and B). Interestingly, treatment of obese mice for 2 weeks with myriocin reversed this reduction in exercise capacity (Fig. 3A and B). This improvement in exercise capacity observed in obese mice treated with myriocin can be explained by enhanced whole-body oxygen consumption rates compared with their control counterparts (Fig. 4A–C). In addition, we observed greater citrate synthase activity in gastrocnemius muscle of obese mice treated with myriocin (Fig. 4D). Furthermore, protein expression of peroxisome proliferator-activated receptor- γ coactivator-1 α (PGC1 α), a transcriptional coactivator that plays a key role in regulating a number of genes involved in energy metabolism (18), showed a trend toward a reduction in control-treated DIO

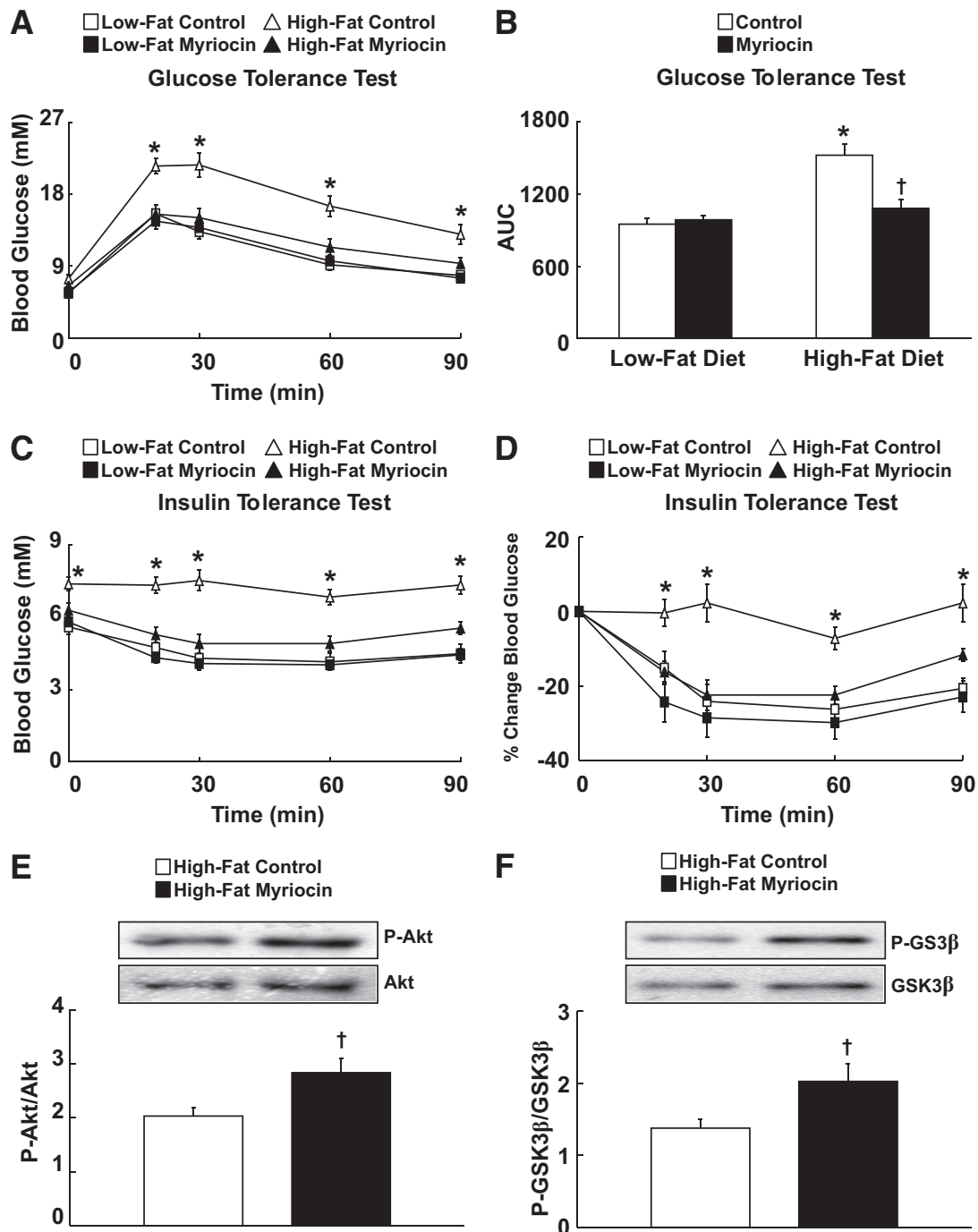


FIG. 1. Inhibition of serine palmitoyl transferase 1 (SPT1) reverses high-fat diet-induced insulin resistance and improves insulin signaling. **A:** Glucose tolerance test in low-fat-fed and obese insulin-resistant mice treated with either vehicle control or myriocin. **B:** Area under the curve during the glucose tolerance test. **C:** Insulin tolerance test in low-fat diet and obese insulin-resistant mice treated with either vehicle control or myriocin. **D:** Percent change in blood glucose levels during the insulin tolerance test. **E:** Insulin-stimulated Akt phosphorylation at serine 473, and **(F)** GSK3 β phosphorylation at serine 9 in gastrocnemius muscle of obese insulin-resistant mice treated with either vehicle control or myriocin. Values represent mean \pm SE ($n = 8-12$ for **A-D**; $n = 4$ for **E** and **F**). Differences were determined using either a two-tailed Student t test or a two-way ANOVA followed by a Bonferroni post hoc analysis. * $P < 0.05$, significantly different from all other groups. † $P < 0.05$, significantly different from the high-fat diet control mice.

mice ($P = 0.077$) that was not apparent in myriocin-treated DIO mice (Fig. 4E). Furthermore, we also demonstrate that pretreatment with myriocin increases citrate synthase activity in C2C12 myotubes exposed to 1.0 mmol/l palmitate for 16 h (Fig. 4F). These observations illustrate improvements in mitochondrial function, possibly explaining why exercise capacity and whole-body oxygen consumption rates were enhanced in this group.

Metabolic profiling of mice provided further insight with regards to mitochondrial function in obese, insulin-resistant mice, as control-treated DIO mice had a significant increase in long-chain acyl carnitine esters versus their lean counterparts (Table 3), indicative of mitochondrial overload and the incomplete oxidation of fatty acids (19). However, the accumulation of long-chain acyl carnitine esters in myriocin-treated DIO mice was even greater

TABLE 2

Effect of myriocin on body and tissue weight, and plasma glucose and insulin levels in lean and obese mice

	LF control	LF myriocin	HF control	HF myriocin
Body weight (g)	29.80 ± 0.20	28.26 ± 0.77	43.73 ± 0.98*	41.77 ± 0.94*
Fed blood glucose (mM)	8.35 ± 0.39	7.74 ± 0.41	12.39 ± 1.86*	8.65 ± 0.55
Fasted blood glucose (mM)	6.24 ± 0.26	6.29 ± 0.22	7.44 ± 0.49*	6.26 ± 0.22†
Fasted plasma insulin (ng/ml)	0.32 ± 0.02	0.42 ± 0.02	3.95 ± 0.30*	4.73 ± 0.83*
Liver weight (g)	1.41 ± 0.04	1.23 ± 0.04	1.63 ± 0.10	1.32 ± 0.06†
Abdominal fat weight (g)	0.43 ± 0.06	0.71 ± 0.28	1.53 ± 0.17*	1.51 ± 0.10*

Values reported are from $n = 5-11$ mice. Differences were determined using a two-way ANOVA followed by Bonferroni post hoc analysis. *Significantly different from the low-fat counterpart; †Significantly different from high-fat control. LF, low-fat diet; HF, high-fat diet.

(Table 3). This suggests that incomplete fatty acid oxidation rates were even more pronounced in the myriocin-treated DIO mice, but these animals also had a significant reduction in short-chain acyl carnitine ester content (Table 3), which is consistent with long-chain acyl-CoA dehydrogenase inhibition and reduced oxidation of long-chain fatty acids.

Inhibition of de novo ceramide synthesis via pharmacological inhibition of SPT1 reverses diet-induced impairments on heat production with no effect on animal activity. After 3 weeks of treatment with myriocin, in vivo heat production and ambulatory activity were assessed in our CLAMS apparatus. Paralleling our observations with regard to whole-body oxygen consumption rates, obesity caused a decline in whole-body heat production that was reversed by myriocin treatment (supplementary Fig. 5A and B). Moreover, obesity-induced insulin resistance was associated with reductions in physical activity that were not altered by myriocin treatment (supplementary Fig. 5C-E).

Inhibition of de novo ceramide synthesis via pharmacological inhibition of SPT1 has no effect on the obesity-associated increase of long-chain acyl-CoA and DAG accumulation in muscle, but significantly elevates TAG levels. Investigation of the lipid metabolite profile in gastrocnemius muscle demonstrated that chronic high-fat feeding increased long-chain acyl-CoA, ceramide and DAG content, but only a trend to an increase in TAG content was observed (Fig. 5A-D). Treatment with myriocin in obese mice increased gastrocnemius TAG

content in comparison to their low-fat counterparts, but did not change the DIO-associated rise in long-chain acyl-CoA and DAG content, and as expected, resulted in a dramatic reduction in ceramide content (Fig. 5A-D). These results suggest a key role for ceramide in mediating skeletal muscle insulin resistance, and indicate that the other lipid metabolites possibly may not be as important in the insulin-resistance development. Further support for this statement is seen with the positive correlation between ceramide content and the area under the curve during the glucose tolerance test, whereas no correlation was observed with any of the other lipid metabolites (Fig. 5E-H). Interestingly, in a previous study, we showed that mice deficient for malonyl CoA decarboxylase (MCD^{-/-}) are protected from obesity-induced glucose intolerance and insulin resistance, which was associated with a reduction in incomplete fatty acid oxidation rates (19). In this study we show that these same MCD^{-/-} mice do not accumulate ceramide in their gastrocnemius muscle after 12 weeks of high-fat feeding (Fig. 6), although they did accumulate other lipid metabolites such as long-chain acyl-CoA (19).

Inhibition of de novo ceramide synthesis via pharmacological inhibition of SPT1 prevents the development of insulin resistance in leptin receptor deficient type 2 diabetes *db/db* mice. To determine if ceramides may also be involved in genetic forms of insulin resistance and type 2 diabetes, we treated leptin receptor deficient (*db/db*) mice with myriocin to see if we could prevent the progression of insulin resistance in these animals. We split

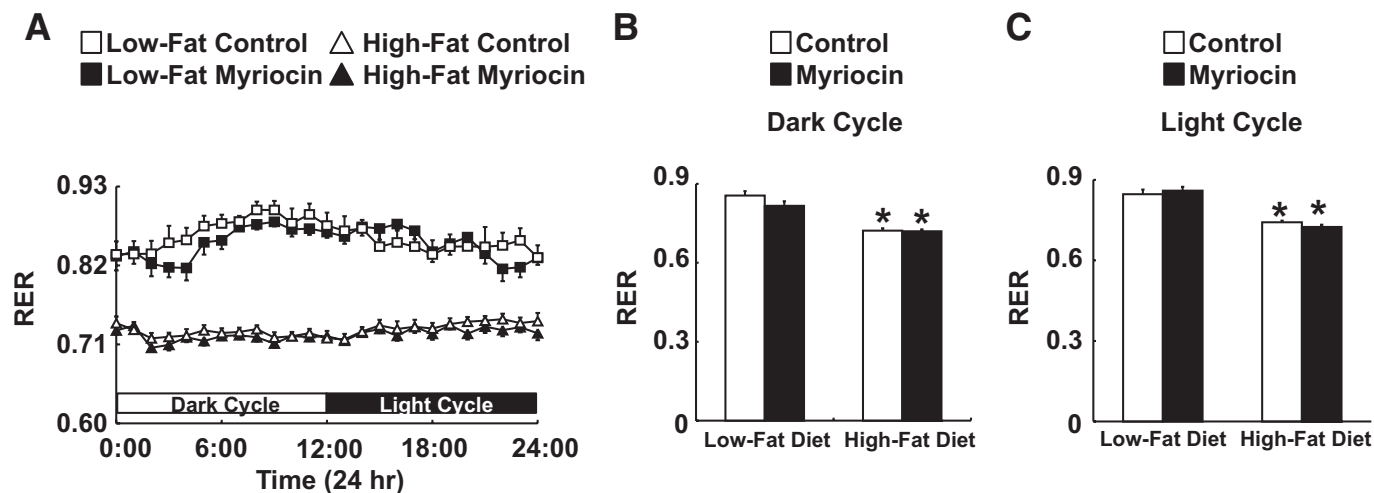


FIG. 2. Substrate preference in lean and obese mice. Twenty-four-hour (A), dark cycle (B), and light cycle respiratory exchange ratio (C) in low-fat-fed and obese insulin-resistant mice treated with either vehicle control or myriocin. Values represent mean ± SE ($n = 8-12$). Differences were determined using a two-way ANOVA followed by a Bonferroni post hoc analysis. * $P < 0.05$, significantly different from the low-fat diet counterpart.

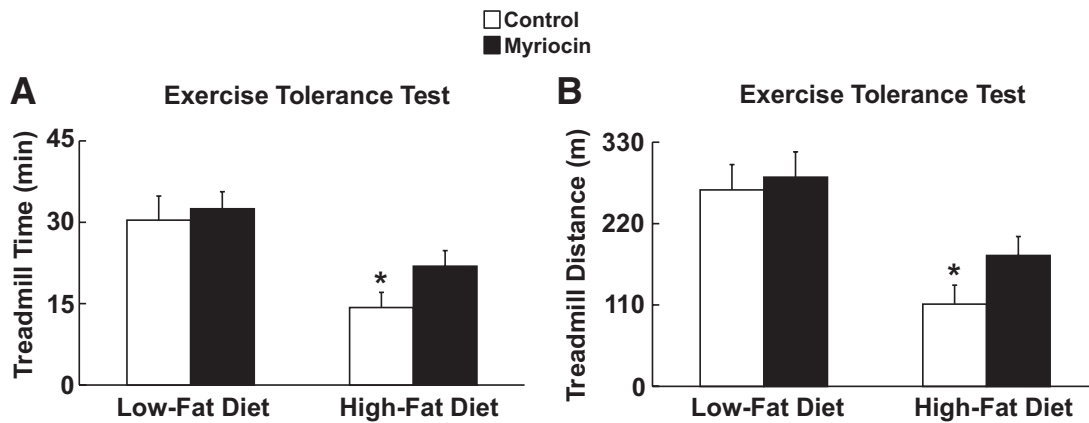


FIG. 3. Myriocin treatment reverses the impairment in aerobic exercise capacity caused by DIO. Time (A) and distance (B) during an exercise capacity challenge on a running treadmill. Values represent mean \pm SE ($n = 8-12$). Differences were determined using a two-way ANOVA followed by a Bonferroni post hoc analysis. * $P < 0.05$, significantly different from the low-fat diet counterpart.

db/db mice at 6 weeks of age into two groups, and ensured that there were no differences in glucose tolerance before initiating treatment with myriocin (Fig. 6A). Both the *db/db* control and myriocin-treated groups experienced similar body weight increases after 2 weeks of treatment (data not shown), however, although the *db/db* control group became glucose intolerant, the *db/db* group treated with myriocin did not (Fig. 7B and C). Fasting blood glucose levels were also significantly lower in the *db/db* mice treated with myriocin, and although their response to insulin was delayed, myriocin-treated *db/db* mice demonstrated lower blood glucose levels at nearly all time points during an insulin tolerance test (Fig. 7D–F). Placing these animals in the CLAMS apparatus yielded a profile similar to that of the DIO mice. The *db/db* controls had a lower RER in the dark cycle than *db/+* lean mice, and had lower whole-body oxygen consumption rates and ambulatory activity, but no change in overall heat production; interestingly, myriocin treatment of *db/db* mice did not restore any of these altered parameters in *db/db* controls, except for a restoration of whole-body oxygen consumption rates during the light cycle (Fig. 8A–D). Examination of the lipid metabolite profile revealed that TAG and long-chain acyl-CoA levels were elevated in gastrocnemius muscle of *db/db* controls versus *db/+* lean mice, whereas, unexpectedly, DAG and ceramide levels were similar between the two groups (Fig. 8E–H). Myriocin treatment of *db/db* mice had no effect on TAG, long-chain acyl-CoA, or DAG levels in gastrocnemius muscle versus *db/db* control mice, but did lead to a dramatic reduction in ceramide levels (Fig. 8E–H). Insulin-stimulated Akt and GSK3 β phosphorylation were also depressed in *db/db* control versus *db/+* lean mice, but showed an improvement in *db/db* mice treated with myriocin (Fig. 8I and J).

DISCUSSION

Our results show that inhibition of SPT1 reduces de novo ceramide synthesis in muscle, which has novel effects on whole-body energy metabolism and is associated with a profound reversal of glucose intolerance and insulin resistance induced by chronic high-fat feeding. Furthermore, we show that these improvements are dissociated from the other lipid metabolites believed to play a role in the development of insulin resistance. Interestingly, obesity-induced insulin resistance in mice is associated with a detriment in aerobic exercise capacity and whole-body

oxygen consumption rates, both of which are partially reversed via SPT1 inhibition.

Previous studies have postulated that skeletal muscle insulin resistance is caused by the intramyocellular cytosolic accumulation of lipid metabolites (TAG, long-chain acyl-CoA, DAG, ceramide, etc.) that negatively impact the insulin signaling cascade (2–4,8,20,21). In particular, long-chain acyl-CoA and DAG have received considerable attention because of their ability to activate the classic/novel protein kinase C signaling cascade, which can phosphorylate insulin receptor substrate proteins on serine residues, preventing their activation via the insulin receptor (4,5,8,21–23). It is important to note, however, that most (~95%) acyl-CoA esters are located inside the mitochondria (24,25), suggesting that if long-chain acyl-CoA accumulation does play a role toward insulin resistance development, it is possible that mitochondrial, as opposed to cytosolic long-chain acyl-CoA, is the primary contributor. Although TAG has been shown in numerous studies to be elevated in muscle in association with the development of insulin resistance, recent studies have shown that TAG may actually serve as a buffer, protecting the muscle against the accumulation of the more reactive lipid metabolite species (10,11).

In regards to ceramide, data are mixed with its role in insulin resistance development, because in some studies, ceramide accumulation is not evident in muscle (5,26), and in other studies where accumulation does occur, the relative increase in the ceramide pool is not that large (12,27). However, a recent study by Holland et al. (12) has shed some light on this issue, as they demonstrated that ceramide accumulation in muscle is dependent on the type of diet fed to the animals. In particular, saturated fatty acids drive de novo ceramide synthesis in muscle via SPT1, whereas unsaturated fatty acids cause insulin resistance via other mechanisms (12). Such findings may potentially explain why ceramide accumulation is not observed in studies of insulin resistance where the model employed is a lipid infusion that consists primarily of unsaturated fatty acids (22). Furthermore, Holland et al. (12) showed in their study that preventing de novo synthesis of ceramide via SPT1 inhibition with myriocin prevented the development of glucose intolerance in obese Zucker rats, and prevented the palmitate-induced inhibition of insulin-stimulated 2-deoxyglucose uptake in isolated soleus muscle.

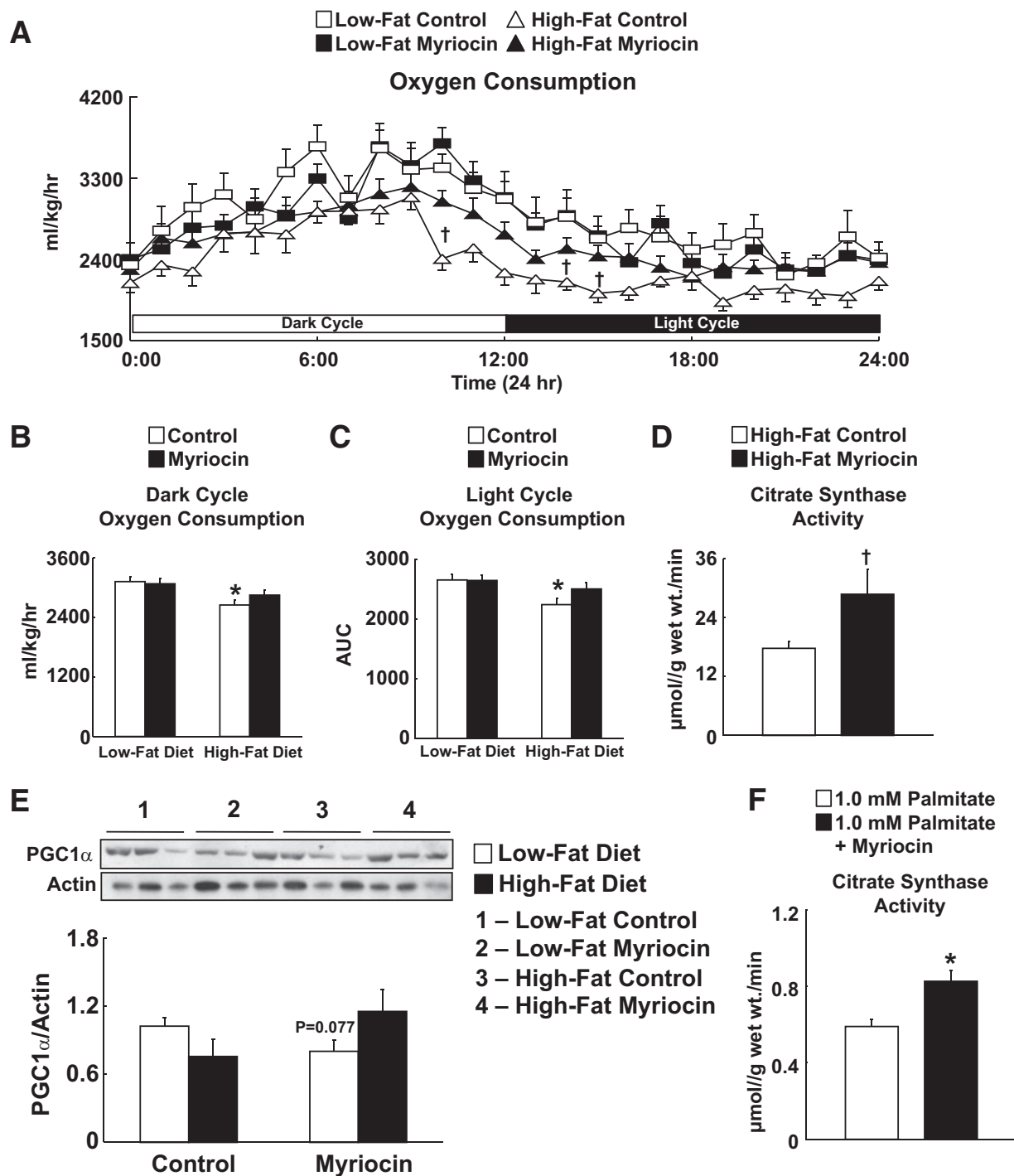


FIG. 4. Myriocin treatment reverses the impairment in whole-body oxygen consumption rates caused by DIO. *A–C*: Twenty-four hour (*A*), dark cycle (*B*), and light cycle (*C*) whole-body oxygen consumption assessment in low-fat diet and obese insulin-resistant mice treated with either vehicle control or myriocin. *D*: Gastrocnemius muscle citrate synthase activity in vehicle control and myriocin-treated DIO mice. *E*: PGC1 α expression in low-fat diet and obese insulin-resistant mice treated with either vehicle control or myriocin. *F*: Citrate synthase activity in vehicle control and myriocin-pretreated C2C12 skeletal muscle myotubes exposed to 1.0 mmol/l palmitate for 16 h. Values represent mean \pm SE ($n = 5–12$). Differences were determined using either a two-tailed Student *t* test or a two-way ANOVA followed by a Bonferroni post hoc analysis. * $P < 0.05$, significantly different from the low-fat diet counterpart. † $P < 0.05$, significantly different from the high-fat diet control mice. AUC, area under the curve.

Another recent study by Yang et al. (28) also reported positive findings with myriocin treatment in leptin-deficient and DIO mice, providing further support that ceramide plays a key role in the development of insulin resistance. Interestingly, these authors also observed a weight loss effect due to myriocin treatment that we did not observe in our studies. However, the authors in this

study used a much longer treatment than ours (8 vs. 4 weeks), and noted that they did not observe a weight loss effect until later in the treatment period. Furthermore, 3 weeks of myriocin treatment in DIO mice improved hyperglycemia and whole-body oxygen consumption rates in their mice, despite no change in body weight compared with control-treated DIO mice, which is consistent with

TABLE 3

Metabolic profiling of gastrocnemius muscle from lean and obese mice treated with either vehicle control or myriocin

	LF control	LF myriocin	HF control	HF myriocin
Short-chain acylcarnitines	2,488 ± 78	2,481 ± 187	2,215 ± 147	1,704 ± 131*
Medium-chain acylcarnitines	18.2 ± 3.5	15.9 ± 4.6	23.5 ± 2.7	22.0 ± 3.4
Long-chain acylcarnitines	56.9 ± 9.3	67.8 ± 19.7	142.5 ± 8.6*	292.3 ± 62.7*†
Short-chain/long-chain acylcarnitine ratio	47.9 ± 5.4	59.81 ± 16.6	18.6 ± 5.0*	7.7 ± 2.2*†

Values reported are in pmol/mg protein from $n = 6$ mice. Differences were determined using a two-way ANOVA followed by Bonferroni post hoc analysis. *Significantly different from the LF counterpart. †Significantly different from high-fat control. LF, low-fat diet; HF, high-fat diet.

our results in DIO mice treated with myriocin for 2 weeks. Yang et al. also observed a dramatic reduction in hepatic steatosis that is consistent with our observations in regards to hepatic TAG content.

Our study adds further support to the studies examining the role of ceramide in mediating insulin resistance (12,28) by illustrating the potential for targeting SPT1 as a treatment against insulin resistance. Our data highlight that targeting SPT1 can be used to reverse insulin resistance in DIO. Moreover, by examining other lipid metabolites such as TAG, DAG, long-chain acyl-CoA, and acyl carnitine content in skeletal muscle, we are able to discern important differences with regard to the relative importance of each metabolite toward the development of skeletal muscle insulin resistance.

Importantly, reductions in skeletal muscle ceramide accumulation may represent a potential explanation for the “exercise paradox” observed in humans. Dube et al. (15) showed that obese, insulin-resistant men placed on an aerobic exercise training regime have elevated intramyocellular lipid and TAG stores. However, marked reductions in muscle ceramide levels are observed, which may explain the enhanced insulin sensitivity of these men. Moreover, Bruce et al. (14) showed that the improved insulin sensitivity observed with exercise training in humans is associated with a drop in muscle ceramide levels, and in particular, the saturated species. Animal studies of exercise have also yielded similar findings, as Dobrzyn et al. (29) showed that exercise training of rats leads to a dramatic drop in the saturated species of ceramide in muscle, which is associated with an enhanced 2-deoxyglucose uptake. In addition, mice overexpressing diacylglycerol acyl transferase in muscle are protected from high-fat-diet-induced insulin resistance and palmitate inhibition of 2-deoxyglucose uptake in isolated muscle, both of which are associated with an elevation of muscle TAG and drop in ceramide levels (10). Our results support these studies, as we show that obese, insulin-resistant mice treated with myriocin had significant increases in intramyocellular TAG, long-chain acyl-CoA, and DAG, but a dramatic drop in ceramide content. Moreover, we observed a positive correlation with ceramide content and glucose intolerance, but not with any of the other lipid metabolites. We believe that with this finding, in the setting of obesity, that ceramide may be more vital to the development of skeletal muscle insulin resistance than the other lipid metabolites. Support for this statement is also evident in culture models of ceramide accumulation, whereby inhibition of SPT1 was able to prevent palmitate-induced insulin resistance in both human and rat L6 myotubes, despite elevated TAG and DAG levels (11,13). Furthermore, a recent study in humans demonstrated that insulin resistant muscle is associated with elevated ceramide content, but no change in DAG content (30). None-

theless, it is also important to note that our measurement of DAG assessed total cellular levels of DAG, and it is possible that differences in plasma membrane DAG were significantly reduced via myriocin treatment. Because DAG at the membrane is believed to be the specific DAG pool responsible for mediating skeletal muscle insulin resistance (3), it will be important for future studies to investigate this in more detail.

One of the most surprising findings of this study was that chronic high-fat feeding resulted in a dramatic decline in whole-body oxygen consumption rates. The majority of studies that have examined the effect of high-fat feeding on whole-body oxygen consumption rates via use of the CLAMS apparatus have reported elevations in oxygen consumption rates (16,17). Although the differences between these studies and ours could be due to the duration or composition of the diet, we propose two possible explanations for this observation of ours. First, it has been reported that obesity-induced insulin resistance causes mitochondrial dysfunction that results from an impairment of fatty acid oxidative capacity (5–8). Although it may be possible that our model of insulin resistance is inducing mitochondrial dysfunction, it is highly unlikely due to impairments in muscle fatty acid oxidative capacity, as the RER values in obese mice reported in this study are very close to 0.7, indicating that these animals have no trouble utilizing fat as an energy source. Nonetheless, other factors, such as mitochondrial content, protein expression of electron transport chain (ETC) complexes, or activity of these complexes, may account for potential mitochondrial dysfunction and the subsequent impairment of oxygen consumption rates observed in obese mice (31,32). However, we did not observe differences in protein expression of cytochrome C of the ETC in any group (data not shown). Second, and just as relevant to the findings of this study, is that obesity-induced insulin resistance has been associated with elevated rates of incomplete fatty acid oxidation, which can arise when rates of fatty acid oxidation are disconnected from TCA cycle activity (19,33,34). This disconnect arises due to the sedentary nature of obese individuals and animals, thus there is no demand for the TCA cycle to upregulate its activity to deal with the increased fatty acid supply that is being utilized as an energy source (19,33,34). If the TCA cycle is unable to accommodate the increasing acetyl CoA coming from fatty acid oxidation, reducing equivalents such as NADH and FADH₂ would not donate their electrons to the complexes of the ETC, accounting for the reduction in oxygen consumption rates.

Our observation of increased accumulation of long-chain acyl carnitine esters in the muscle of DIO mice is thus consistent with elevated rates of incomplete fatty acid oxidation. In contrast, there was an even greater accumulation of long-chain acyl carnitine esters in myri-

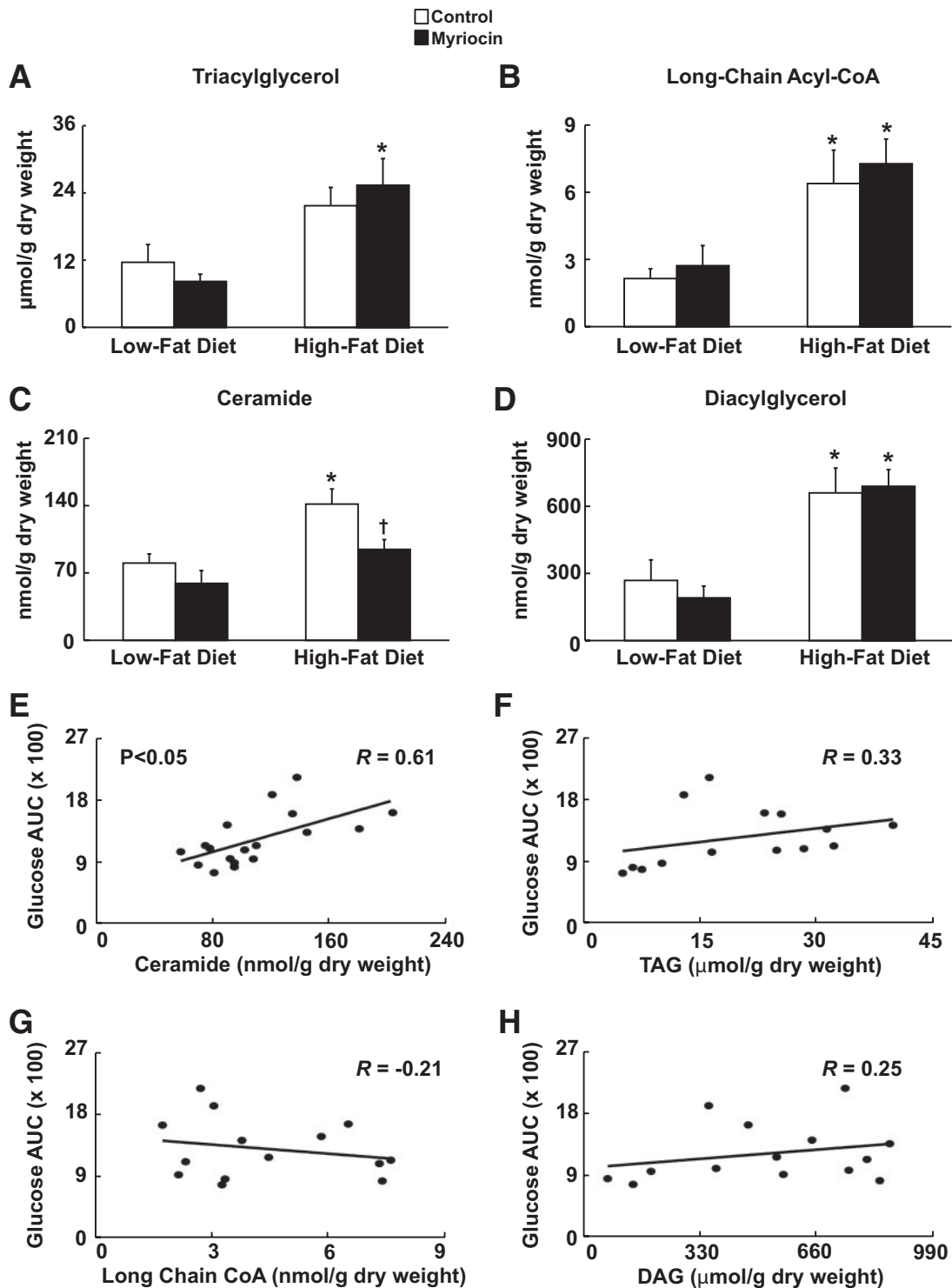


FIG. 5. Inhibition of SPT1 reduces skeletal muscle ceramide levels with no effect on other lipid metabolites. *A–D*: Gastrocnemius triacylglycerol (TAG) (*A*), long-chain acyl-CoA (*B*), ceramide (*C*), and diacylglycerol (*D*) levels in low-fat-fed and obese insulin-resistant mice treated with either vehicle control or myriocin. Values represent mean \pm SE ($n = 4–8$). Differences were determined using a two-way ANOVA followed by Bonferroni post hoc analysis. * $P < 0.05$, significantly different from the low-fat diet counterpart. † $P < 0.05$, significantly different from the high-fat diet control mice. *E–H*: Correlation between the respective areas under the curve during the glucose tolerance test and ceramide (*E*), TAG (*F*), long-chain acyl-CoA (*G*), and diacylglycerol (*H*) content of ($n = 14–18$) samples. Correlation was determined via Pearson correlation test. *R*, multivariate correlation coefficient. AUC, area under the curve.

ocin-treated DIO mice, which at first glance would suggest even greater rates of incomplete fatty acid oxidation in these animals. However, myriocin-treated DIO mice actually had a significant reduction in the content of a number of short-chain acyl carnitine esters, and this, in combination with the rise of long-chain acyl carnitine esters, is

suggestive of long-chain acyl-CoA dehydrogenase and subsequent long-chain fatty acid oxidation inhibition (35). Another piece of indirect support for fatty acid oxidation inhibition with myriocin treatment in DIO mice is the observation that TAG accumulated in the muscle of these animals versus their lean counterparts, but not in control-

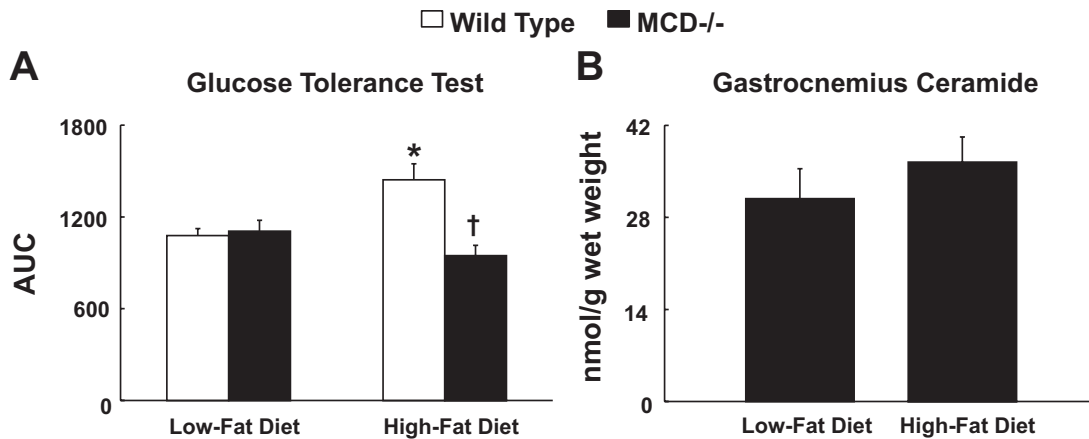


FIG. 6. Malonyl CoA decarboxylase-deficient mice (MCD^{-/-}) do not accumulate skeletal muscle ceramide after 12 weeks of high-fat feeding. **A:** Area under the curve during a glucose tolerance test after 12 weeks of high-fat feeding in wild-type and MCD^{-/-} mice. **B:** Corresponding gastrocnemius ceramide levels in MCD^{-/-} mice after 12 weeks of high-fat feeding. Values represent mean \pm SE ($n = 5-8$). Differences were determined using a two-way ANOVA followed by Bonferroni post hoc analysis. * $P < 0.05$, significantly different from low-fat diet counterpart. † $P < 0.05$, significantly different from the high-fat diet wild-type mice. AUC, area under the curve.

treated DIO mice versus their lean counterparts. A reduction in fatty acid oxidation-derived NADH would decrease NADH/NADPH oxidase activity and subsequent superoxide production in myriocin-treated DIO mice, which would contribute toward their improved mitochondrial function. This improvement in mitochondrial function, coupled together with improvements in glucose metabolism and glucose-derived acetyl CoA production for the TCA cycle,

may contribute to the greater oxygen consumption rates in these animals. Obesity-induced decrements in PGC1 α protein expression might also explain impairments in mitochondrial function (34,36,37), and although not significant, we observed a trend toward a reduction in gastrocnemius PGC1 α protein expression in control-treated DIO mice ($P = 0.077$) that was not evident in myriocin-treated DIO mice. Interestingly, citrulline levels were increased in

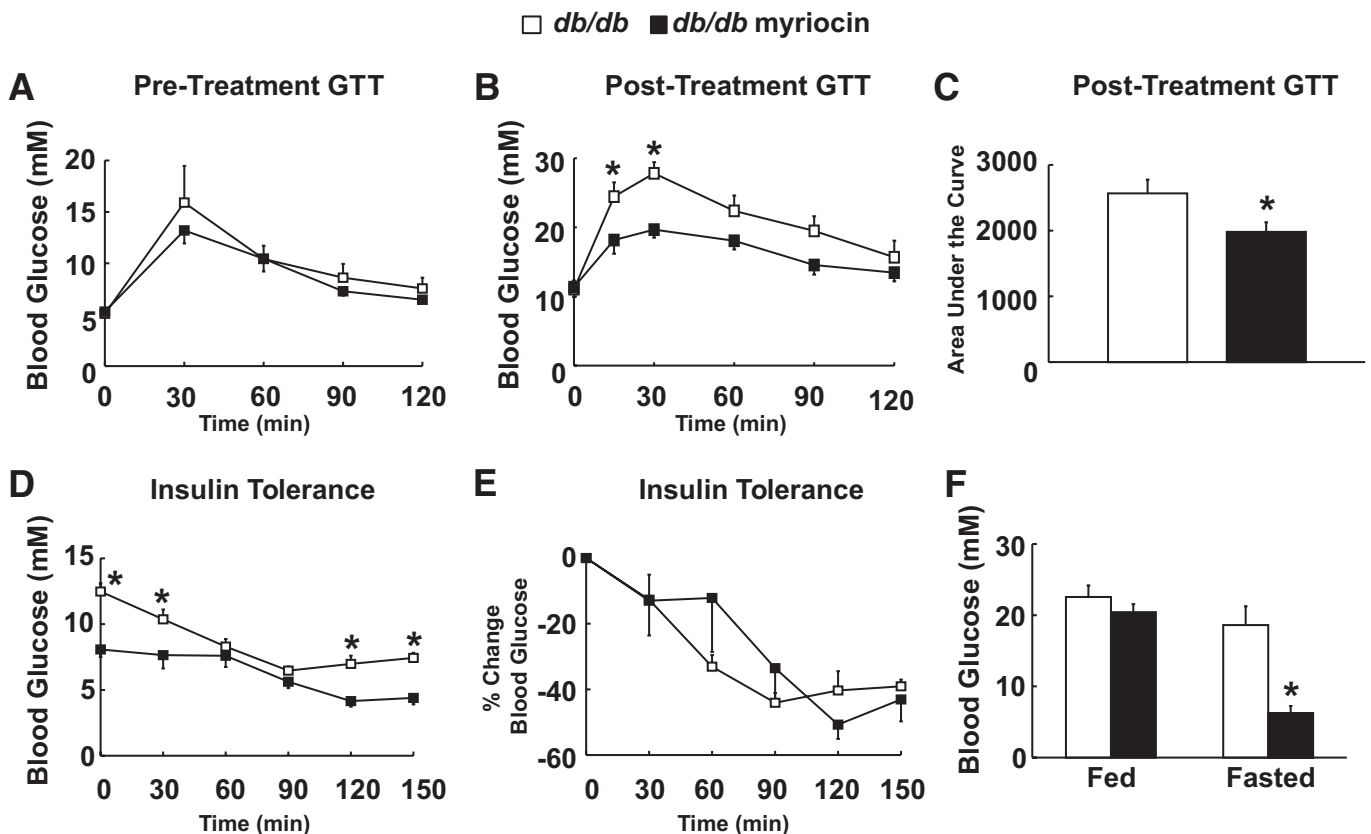


FIG. 7. Prevention of insulin resistance in *db/db* mice via myriocin treatment. **A:** Pretreatment glucose tolerance test (GTT) in *db/db* mice at 6 weeks of age. **B:** GTT in *db/db* mice treated with vehicle control or myriocin. **C:** Respective areas under the curve for the post-treatment GTT in *db/db* mice. **D:** Insulin tolerance test (ITT) in *db/db* mice treated with vehicle control or myriocin. **E:** Percent change in blood glucose levels during the ITT. **F:** Fed and fasted plasma glucose levels in *db/db* mice treated with vehicle control or myriocin. Values represent mean \pm SE ($n = 5-6$). Differences were determined using either a two-tailed Student *t* test, or a one-way or two-way ANOVA followed by Bonferroni post hoc analysis. * $P < 0.05$, significantly different from the *db/db* control mice.

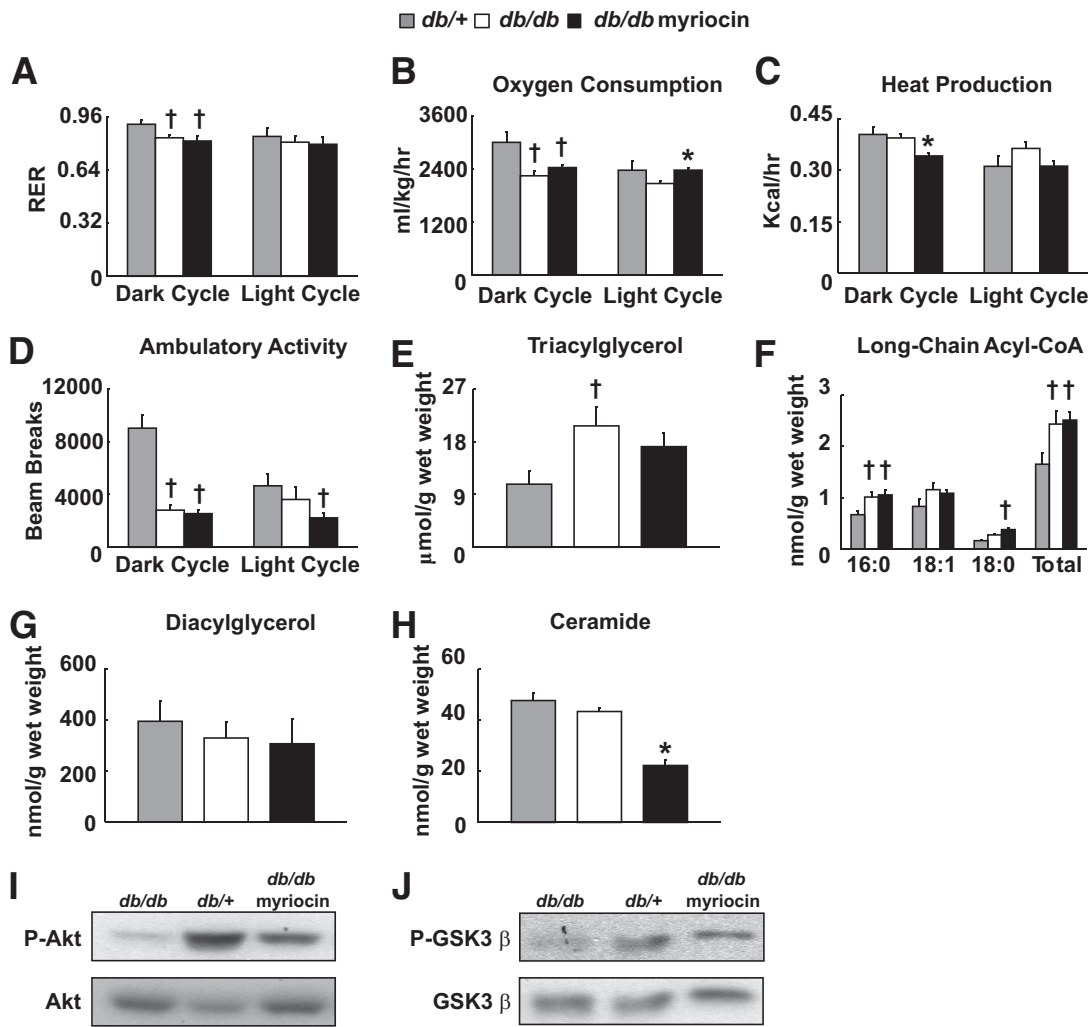


FIG. 8. In vivo metabolic parameters, intramyocellular lipid metabolite profile, and insulin signaling in *db/db* mice treated with myriocin. RER (A), whole-body oxygen consumption (B), heat production (C), and ambulatory activity (D) in *db/+* heterozygous mice, and *db/db* mice treated with vehicle control or myriocin. Gastrocnemius triacylglycerol (E), long-chain acyl-CoA (F), diacylglycerol (G), and ceramide levels (H) in *db/+* heterozygous mice, and *db/db* mice treated with vehicle control or myriocin. I: Insulin stimulated Akt phosphorylation at serine 473, and (J) GSK3β phosphorylation at serine 9 in gastrocnemius muscle of *db/+* heterozygous mice and *db/db* mice treated with vehicle control or myriocin. Values represent mean ± SE (n = 3–5). Differences were determined using either a one-way or two-way ANOVA followed by Bonferroni post hoc analysis. *P < 0.05, significantly different from the *db/db* control mice. †P < 0.05, significantly different from the *db/+* heterozygous mice.

myriocin-treated DIO mice versus their control counterparts (supplementary Fig. 6). A previous study in humans showed that supplementation of citrulline enhances aerobic oxidative metabolism (38), supporting our findings of increased whole-body oxygen consumption rates and greater exercise time in myriocin-treated DIO mice. How myriocin and subsequent SPT1 inhibition would influence skeletal muscle citrulline levels is currently unknown, but is undoubtedly an intriguing avenue for future investigation. In addition, we have previously shown that MCD^{-/-} mice (a genetic model of fatty acid oxidation deficiency) are protected from obesity-induced insulin resistance. Interestingly, we show in this study that these exact same animals do not accumulate ceramide in their muscle after 12 weeks of high-fat feeding, leading to the very intriguing possibility that intramyocellular ceramide accumulation is linked to the mitochondrial dysfunction and enhanced skeletal muscle fatty acid oxidation rates observed in insulin resistance.

A limitation with our interpretation of whole-body oxygen consumption rates is that, unlike human studies, we were unable to normalize our oxygen consumption

rates to lean body mass. It is entirely possible that whole-body oxygen consumption rates were simply lower in DIO mice because of a significant increase in overall adiposity, due to fat mass having a lower metabolic rate than lean body mass. However, the fact that adiposity and body weight were similar between myriocin- and control-treated DIO mice suggests that this would not be a contributing factor to the higher oxygen consumption rates observed in the myriocin-treated DIO mice. Although we believe that the changes accounting for the greater oxygen consumption rates in myriocin-treated DIO mice primarily reflect the muscle, we cannot ignore possible contributions from changes in other peripheral tissues, such as brown adipose tissue and uncoupling protein activity.

The beneficial effects mediated by inhibition of SPT1 and prevention of de novo ceramide synthesis could also arise from liver effects in our animals. Regardless, we did not observe increases in hepatic ceramide content after diet-induced obesity, and myriocin treatment had no effect on insulin-stimulated Akt and GSK3 phosphorylation in obese mice versus their respective con-

trols (supplementary Fig. 7). In support of our liver ceramide observations, recent studies have also shown that high-fat feeding does not increase ceramide content in the liver (39), and increases in hepatic ceramide content via genetic overexpression of either DGAT1 or DGAT2 does not result in any type of insulin resistance or inflammation (40). Moreover, we reported no difference during a pyruvate challenge of fasted, obese, control- or myriocin-treated mice (supplementary Fig. 8), suggesting that gluconeogenic capacity was not different between the two groups and that the liver likely does not play a key role with the improved insulin sensitivity observed in myriocin-treated mice. Regardless, we cannot entirely rule out the possibility that the liver plays a role with the benefit observed during myriocin treatment, as the DIO-associated rise in hepatic TAG content was reversed via myriocin treatment, and thus it will be important for future studies to delineate the role of hepatic SPT1 in greater depth.

Finally, chronic low-grade inflammation has been shown in a number of studies to play a role in causing obesity-induced insulin resistance (41–43). Inflammatory and stress kinases, such as p38 MAPK and JNK, have been proposed to be downstream mediators of this inflammatory effect, as inhibitors of both kinases are able to prevent high-fat diet-induced insulin resistance (9,44–46). Unexpectedly, the phosphorylation status of both p38 MAPK and JNK was not altered by DIO, nor was it altered by myriocin treatment (supplementary Fig. 9), suggesting that inflammation may not play as vital a role in our model of insulin resistance. It may also be possible that inflammation in our model is mediated by some other kinase, such as IKK β (47,48).

With regard to the findings in *db/db* mice, we report very similar findings to what we observed in the obesity-induced insulin-resistant mice, and that treatment with myriocin also yielded a very similar beneficial profile. Interestingly, gastrocnemius ceramide levels, although reduced in myriocin-treated *db/db* mice, did not differ between *db/+* lean and *db/db* control mice. This suggests, at least in this model, that perhaps ceramide metabolites, such as glucosylceramide, are more important in mediating skeletal muscle insulin resistance than ceramide itself (49). Furthermore, the ceramide pool is under a dynamic process of synthesis and degradation (9), and although de novo synthesis of ceramide may be increased in these animals, a simultaneous increase in ceramide degradation would mask out any noticeable change.

In summary, we show that ceramide accumulation in skeletal muscle plays a key role during obesity-induced insulin resistance, whereas the other lipid metabolites, such as TAG, long-chain acyl-CoA, and DAG, may not be as vital. Importantly, inhibition of de novo ceramide synthesis has novel effects on whole-body energy metabolism and is sufficient to reverse obesity-induced whole-body glucose intolerance and insulin resistance. Furthermore, whole-body oxygen consumption rates and exercise capacity in obese mice are improved via inhibition of de novo ceramide synthesis. Last, our finding that muscle ceramide levels are not elevated in *db/db* mice, but that inhibition of de novo ceramide synthesis still prevents their development of insulin resistance, suggests the possibility that ceramide metabolites may also play a role in the progression of this disease.

ACKNOWLEDGMENTS

This study was supported by a grant to G.D.L. from the Canadian Diabetes Association, and the Heart and Stroke Foundation of Alberta. G.D.L. is an Alberta Heritage Foundation for Medical Research Medical Scientist. J.R.U. is a trainee of the Alberta Heritage Foundation for Medical Research and Tomorrow's Research Cardiovascular Health Professionals.

No potential conflicts of interest relevant to this article were reported.

The authors thank the dedicated staff of the University of Alberta Cardiovascular Translational Research Centre High Performance Liquid Chromatography Core Facility for the measurement of lipid metabolites in skeletal muscle, and the University of Alberta Cardiovascular Translational Research Centre Animal Physiology Core Facility for in vivo metabolic assessment via the CLAMS apparatus. The authors also thank Cory Wagg for technical assistance.

REFERENCES

- Kahn SE, Hull RL, Utzschneider KM. Mechanisms linking obesity to insulin resistance and type 2 diabetes. *Nature* 2006;444:840–846
- Muoio DM, Newgard CB. Obesity-Related Derangements in Metabolic Regulation. *Annu Rev Biochem*, 2006
- Savage DB, Petersen KF, Shulman GI. Disordered lipid metabolism and the pathogenesis of insulin resistance. *Physiol Rev* 2007;87:507–520
- Shulman GI. Cellular mechanisms of insulin resistance. *J Clin Invest* 2000;106:171–176
- Choi CS, Savage DB, Abu-Elheiga L, Liu ZX, Kim S, Kulkarni A, Distefano A, Hwang YJ, Reznick RM, Codella R, Zhang D, Cline GW, Wakil SJ, Shulman GI. Continuous fat oxidation in acetyl-CoA carboxylase 2 knock-out mice increases total energy expenditure, reduces fat mass, and improves insulin sensitivity. *Proc Natl Acad Sci U S A* 2007;104:16480–16485
- Steinberg GR, Michell BJ, van Denderen BJ, Watt MJ, Carey AL, Fam BC, Andrikopoulos S, Proietto J, Gorgun CZ, Carling D, Hotamisligil GS, Febbraio MA, Kay TW, Kemp BE. Tumor necrosis factor α -induced skeletal muscle insulin resistance involves suppression of AMP-kinase signaling. *Cell Metab* 2006;4:465–474
- Watt MJ, Dzamko N, Thomas WG, Rose-John S, Ernst M, Carling D, Kemp BE, Febbraio MA, Steinberg GR. CNTF reverses obesity-induced insulin resistance by activating skeletal muscle AMPK. *Nat Med* 2006;12:541–548
- Zhang D, Liu ZX, Choi CS, Tian L, Kibbey R, Dong J, Cline GW, Wood PA, Shulman GI. Mitochondrial dysfunction due to long-chain Acyl-CoA dehydrogenase deficiency causes hepatic steatosis and hepatic insulin resistance. *Proc Natl Acad Sci U S A* 2007;104:17075–17080
- Summers SA. Ceramides in insulin resistance and lipotoxicity. *Prog Lipid Res* 2006;45:42–72
- Liu L, Zhang Y, Chen N, Shi X, Tsang B, Yu YH. Upregulation of myocellular DGAT1 augments triglyceride synthesis in skeletal muscle and protects against fat-induced insulin resistance. *J Clin Invest* 2007;117:1679–1689
- Pickersgill L, Litherland GJ, Greenberg AS, Walker M, Yeaman SJ. Key role for ceramides in mediating insulin resistance in human muscle cells. *J Biol Chem* 2007;282:12583–12589
- Holland WL, Brozinick JT, Wang LP, Hawkins ED, Sargent KM, Liu Y, Narra K, Hoehn KL, Knotts TA, Siesky A, Nelson DH, Karathanasis SK, Fontenot GK, Birnbaum MJ, Summers SA. Inhibition of ceramide synthesis ameliorates glucocorticoid-, saturated-fat-, and obesity-induced insulin resistance. *Cell Metab* 2007;5:167–179
- Powell DJ, Turban S, Gray A, Hajdуч E, Hundal HS. Intracellular ceramide synthesis and protein kinase C ζ activation play an essential role in palmitate-induced insulin resistance in rat L6 skeletal muscle cells. *Biochem J* 2004;382:619–629
- Bruce CR, Thrush AB, Mertz VA, Bezaire V, Chabowski A, Heigenhauser GJ, Dyck DJ. Endurance training in obese humans improves glucose tolerance and mitochondrial fatty acid oxidation and alters muscle lipid content. *Am J Physiol Endocrinol Metab* 2006;291:E99–E107
- Dube JJ, Amati F, Stefanovic-Racic M, Toledo FG, Sauers SE, Goodpaster BH. Exercise-induced alterations in intramyocellular lipids and insulin resistance: the athlete's paradox revisited. *Am J Physiol Endocrinol Metab* 2008;294:E882–E888
- Li JZ, Ye J, Xue B, Qi J, Zhang J, Zhou Z, Li Q, Wen Z, Li P. Cideb regulates

- diet-induced obesity, liver steatosis, and insulin sensitivity by controlling lipogenesis and fatty acid oxidation. *Diabetes* 2007;56:2523–2532
17. Seth A, Steel JH, Nichol D, Pocock V, Kumaran MK, Fritah A, Mobberley M, Ryder TA, Rowlerson A, Scott J, Poutanen M, White R, Parker M. The transcriptional corepressor RIP140 regulates oxidative metabolism in skeletal muscle. *Cell Metab* 2007;6:236–245
 18. Handschin C, Spiegelman BM. The role of exercise and PGC1alpha in inflammation and chronic disease. *Nature* 2008;454:463–469
 19. Koves TR, Ussher JR, Noland RC, Slentz D, Mosedale M, Ilkayeva O, Bain J, Stevens R, Dyck JR, Newgard CB, Lopaschuk GD, Muoio DM. Mitochondrial overload and incomplete fatty acid oxidation contribute to skeletal muscle insulin resistance. *Cell Metab* 2008;7:45–56
 20. Holland WL, Knotts TA, Chavez JA, Wang LP, Hoehn KL, Summers SA. Lipid mediators of insulin resistance. *Nutr Rev* 2007;65:S39–46
 21. Chubalin AV, Leng Y, Vieira E, Krook A, Bjornholm M, Long YC, Kotova O, Zhong Z, Sakane F, Steiler T, Nylan C, Wang J, Laakso M, Topham MK, Gilbert M, Wallberg-Henriksson H, Zierath JR. Downregulation of diacylglycerol kinase delta contributes to hyperglycemia-induced insulin resistance. *Cell* 2008;132:375–386
 22. Kim JK, Gimeno RE, Higashimori T, Kim HJ, Choi H, Punreddy S, Mozell RL, Tan G, Stricker-Krongrad A, Hirsch DJ, Fillmore JJ, Liu ZX, Dong J, Cline G, Stahl A, Lodish HF, Shulman GI. Inactivation of fatty acid transport protein 1 prevents fat-induced insulin resistance in skeletal muscle. *J Clin Invest* 2004;113:756–763
 23. Morino K, Neschen S, Bilz S, Sono S, Tsigiriotis D, Reznick RM, Moore I, Nagai Y, Samuel V, Sebastian D, White M, Philbrick W, Shulman GI. Muscle-specific IRS-1 Ser->Ala transgenic mice are protected from fat-induced insulin resistance in skeletal muscle. *Diabetes* 2008;57:2644–2651
 24. Idell-Wenger JA, Grotzmann LW, Neely JR. Coenzyme A and carnitine distribution in normal and ischemic hearts. *J Biol Chem* 1978;253:4310–4318
 25. Robishaw JD, Neely JR. Coenzyme A metabolism. *Am J Physiol* 1985;248:E1–E9
 26. Skovbro M, Baranowski M, Skov-Jensen C, Flint A, Dela F, Gorski J, Helge JW. Human skeletal muscle ceramide content is not a major factor in muscle insulin sensitivity. *Diabetologia* 2008;51:1253–1260
 27. Turinsky J, O'Sullivan DM, Bayly BP. 1,2-Diacylglycerol and ceramide levels in insulin-resistant tissues of the rat *in vivo*. *J Biol Chem* 1990;265:16880–16885
 28. Yang G, Badeanlou L, Bielawski J, Roberts AJ, Hannun YA, Samad F. Central role of ceramide biosynthesis in body weight regulation, energy metabolism, and the metabolic syndrome. *Am J Physiol Endocrinol Metab* 2009;297:E211–E224
 29. Dobrzyn A, Gorski J. Ceramides and sphingomyelins in skeletal muscles of the rat: content and composition. Effect of prolonged exercise. *Am J Physiol Endocrinol Metab* 2002;282:E277–E285
 30. Coen PM, Dube JJ, Amati F, Stefanovic-Racic M, Ferrell RE, Toledo FG, Goodpaster BH. Insulin resistance is associated with higher intramyocellular triglycerides in type I but not type II myocytes concomitant with higher ceramide content. *Diabetes* 59:80–88
 31. Bonnard C, Durand A, Peyrol S, Chanseume E, Chauvin MA, Morio B, Vidal H, Rieusset J. Mitochondrial dysfunction results from oxidative stress in the skeletal muscle of diet-induced insulin-resistant mice. *J Clin Invest* 2008;118:789–800
 32. Sparks LM, Xie H, Koza RA, Mynatt R, Hulver MW, Bray GA, Smith SR. A high-fat diet coordinately downregulates genes required for mitochondrial oxidative phosphorylation in skeletal muscle. *Diabetes* 2005;54:1926–1933
 33. Muoio DM, Newgard CB. Mechanisms of disease: molecular and metabolic mechanisms of insulin resistance and beta-cell failure in type 2 diabetes. *Nat Rev Mol Cell Biol* 2008;9:193–205
 34. Koves TR, Li P, An J, Akimoto T, Slentz D, Ilkayeva O, Dohm GL, Yan Z, Newgard CB, Muoio DM. Peroxisome proliferator-activated receptor-gamma co-activator 1alpha-mediated metabolic remodeling of skeletal myocytes mimics exercise training and reverses lipid-induced mitochondrial inefficiency. *J Biol Chem* 2005;280:33588–33598
 35. Thyfault JP, Cree MG, Zheng D, Zwetsloot JJ, Tapscott EB, Koves TR, Ilkayeva O, Wolfe RR, Muoio DM, Dohm GL. Contraction of insulin-resistant muscle normalizes insulin action in association with increased mitochondrial activity and fatty acid catabolism. *Am J Physiol Cell Physiol* 2007;292:C729–C739
 36. Muoio DM, Koves TR. Skeletal muscle adaptation to fatty acid depends on coordinated actions of the PPARs and PGC1 alpha: implications for metabolic disease. *Appl Physiol Nutr Metab* 2007;32:874–883
 37. Spiegelman BM. Transcriptional control of mitochondrial energy metabolism through the PGC1 coactivators. *Novartis Found Symp* 287:60–63; discussion 63–69, 2007
 38. Bendahan D, Mattei JP, Ghattas B, Confort-Gouy S, Le Guern ME, Cozzone PJ. Citrulline/malate promotes aerobic energy production in human exercising muscle. *Br J Sports Med* 2002;36:282–289
 39. Matsuzaka T, Shimano H, Yahagi N, Kato T, Atsumi A, Yamamoto T, Inoue N, Ishikawa M, Okada S, Ishigaki N, Iwasaki H, Iwasaki Y, Karasawa T, Kumadaki S, Matsui T, Sekiya M, Ohashi K, Hasty AH, Nakagawa Y, Takahashi A, Suzuki H, Yatoh S, Sone H, Toyoshima H, Osuga J, Yamada N. Crucial role of a long-chain fatty acid elongase, Elovl6, in obesity-induced insulin resistance. *Nat Med* 2007;13:1193–1202
 40. Monetti M, Levin MC, Watt MJ, Sajjan MP, Marmor S, Hubbard BK, Stevens RD, Bain JR, Newgard CB, Farese RV, Sr, Hevener AL, Farese RV, Jr. Dissociation of hepatic steatosis and insulin resistance in mice overexpressing DGAT in the liver. *Cell Metab* 2007;6:69–78
 41. Hotamisligil GS. Inflammation and metabolic disorders. *Nature* 2006;444:860–867
 42. Weisberg SP, McCann D, Desai M, Rosenbaum M, Leibel RL, Ferrante AW, Jr. Obesity is associated with macrophage accumulation in adipose tissue. *J Clin Invest* 2003;112:1796–1808
 43. Serino M, Menghini R, Fiorentino L, Amoruso R, Mauriello A, Lauro D, Sbraccia P, Hribal ML, Lauro R, Federici M. Mice heterozygous for tumor necrosis factor-alpha converting enzyme are protected from obesity-induced insulin resistance and diabetes. *Diabetes* 2007;56:2541–2546
 44. de Alvaro C, Teruel T, Hernandez R, Lorenzo M. Tumor necrosis factor alpha produces insulin resistance in skeletal muscle by activation of inhibitor kappaB kinase in a p38 MAPK-dependent manner. *J Biol Chem* 2004;279:17070–17078
 45. Hirosumi J, Tuncman G, Chang L, Gorgun CZ, Uysal KT, Maeda K, Karin M, Hotamisligil GS. A central role for JNK in obesity and insulin resistance. *Nature* 2002;420:333–336
 46. O'Keefe MP, Perez FR, Kinnick TR, Tischler ME, Henriksen EJ. Development of whole-body and skeletal muscle insulin resistance after one day of hindlimb suspension. *Metabolism* 2004;53:1215–1222
 47. Herschkovitz A, Liu YF, Ilan E, Ronen D, Boura-Halfon S, Zick Y. Common inhibitory serine sites phosphorylated by IRS-1 kinases, triggered by insulin and inducers of insulin resistance. *J Biol Chem* 2007;282:18018–18027
 48. Austin RL, Rune A, Bouzakri K, Zierath JR, Krook A. siRNA-mediated reduction of inhibitor of nuclear factor-kappaB kinase prevents tumor necrosis factor-alpha-induced insulin resistance in human skeletal muscle. *Diabetes* 2008;57:2066–2073
 49. Aerts JM, Ottenhoff R, Powlson AS, Grefhorst A, van Eijk M, Dubbelhuis PF, Aten J, Kuipers F, Serlie MJ, Wenekes T, Sethi JK, O'Rahilly S, Overkleeft HS. Pharmacological inhibition of glucosylceramide synthase enhances insulin sensitivity. *Diabetes* 2007;56:1341–1349